Linear and nonlinear optical properties of fullerenes in solid state materials

Giovanna Brusatin*[a] and Raffaella Signorini[b]

[a]*Department of Mechanical Engineering, University of Padova, Materials Section, via Marzolo 9, 35131 Padova, Italy*
[b]*Department of Physical Chemistry, University of Padova, via Loredan 2, 35131 Padova, Italy*

Fullerenes containing nanocomposite materials for optical applications have attracted the attention of many different research groups during the last few years.
Great effort has been devoted to finding appropriate solid state materials allowing the inclusion of fullerenes: among them, polymeric, sol–gel and porous matrices have been largely investigated. Particular emphasis has been placed on the synthesis of these nanostructured materials incorporating fullerenes to reach the best control of fullerene interactions in different environments and higher fullerene dispersions in solid environments.

1. Introduction

An important topic in photonic nanocomposite material science is the design and synthesis of functional materials, which simultaneously allow one to satisfy several characteristics to reach the specific required optical properties and performances.

Their study is currently one of the most active fields of research, and great efforts have been made, during the last few years, in the design of organic systems with nonlinear optical (NLO) properties, such as molecules and polymers with π-conjugated electron systems. More recent progress in this research has been the development of appropriate solid state materials doped with optically active organic molecules.

In particular, fullerene, widely studied since 1990, acts as a functional molecule and its incorporation in a solid state matrix endow the solid material with the fullerene properties if proper control of the microstructure at a nanometric level is achieved. In fact, depending on whether fullerenes are molecularly dispersed, in nanoclusters or a fullerene molecule–matrix interaction occurs, different properties and performances are obtained. Third order nonlinearity, optical limiting (OL), second harmonic generation and photoluminescence (PL) are among the main properties deriving from the photophysical properties of fullerene molecules or confined clusters and can be strongly modified, depending on which nanostructured material is considered.

Photophysical properties deriving from an almost unitary quantum yield for triplet formation are extremely dependent on the environment of the molecule; in fact, a consequence of C_{60} aggregation is the decreasing of this yield. Perturbation of the fullerene molecular orbitals can derive from interactions with the surrounding solid medium and can strengthen the luminescence emission which is otherwise weak. For this reason, an accurate choice and preparation of the nanostructured fullerene-containing material is necessary to preserve the molecularly dispersed state or control the environmental and aggregation effects of C_{60} in order to make these materials useful for specific optical applications.

The aim of this review is to discuss such examples of nanocomposite materials with linear and nonlinear optical properties transferred to the particular host matrix by the fullerene molecule, in particular evidencing when fullerene-environment interactions play a major role in determining the final optical features of the solid material.

Particular regard will be devoted to solid state systems where the properties can be ascribed to the individual fullerene molecule because weak interactions with the solid medium can be reasonably disregarded. In this case, several examples of OL applications are found in the literature and efforts to develop syntheses of materials that allows fullerene molecular dispersion in solid matrices will be described. In this context, sol–gel based materials incorporating fullerenes play a remarkable role and are thus described in some depth.

The study of the influence of a solid environment on fullerene molecules, the nature of the different excited states involved, and their relaxation dynamics in these matrices are indispensable for the understanding and determines the possibility of optimizing the optoelectronic properties of fullerene doped nanostructured materials.

This review is organized as follows. The optical properties of fullerenes and fullerene derivatives are described in Section 2, with particular regard to the OL properties and the PL effects.

Section 3 reports a general discussion of polymeric and sol–gel matrices, useful for the incorporation of fullerenes. These matrices may enhance the nonlinear properties, as shown in Section 4, where strong interactions between fullerenes and solid state systems make charge transfer processes useful, both for OL applications and photoluminescence effects. When aggregates, instead of isolated molecules, are formed, depending on the nanocomposite process synthesis, optical properties are affected; this is described in Section 5. Finally, Section 6 reports an overview of investigated nanostructured materials with a good dispersion of dye in the host matrix, in the last case the nonlinear properties of the embedded dye are the same as in solution.

2. Fullerenes: linear and nonlinear optical properties and optical limiting

Fullerene-C_{60} was discovered in 1985 by H. W. Kroto *et al.*,[1] but only in 1990 was it first synthesized in large quantities by W. Krätschmer *et al.*[2]. From that moment it has been intensively studied in order to investigate its linear and nonlinear optical properties.[3–9]

Fullerene is a black crystalline solid, insoluble in polar

DOI: 10.1039/b202399g

solvents and soluble in aromatic solvents, like benzene or toluene, or in CS_2. It shows a remarkable chemical reactivity, which has allowed the synthesis of a wide variety of fullerene derivatives. These derivatives may exhibit increased solubility in common solvents and functional units appropriate for further processing. Pristine C_{60} is a molecule of high symmetry, with π-electrons delocalised along the whole 3-D structure These properties make C_{60} an interesting material in the nonlinear optical field. It also shows a wide variety of uncommon physical properties ranging from optical limiting[10] to superconductivity[11,12] and photoconductivity.[13] With fullerene derivatives the large symmetry of C_{60} is broken by the presence of side groups, but optical properties still persist or, in some cases, are modified into more favorable ones.

Optical properties of fullerene and fullerene derivatives have been firstly studied in solutions. The linear absorption spectrum of C_{60} shows a strong absorption in the UV region and a very weak absorption in the visible range.[3] With mono-adduct fullerene derivatives the linear absorption spectrum is slightly modified in the visible range: two new peaks, a sharp peak around 430 nm and a broader peak around 700 nm, appear. Fullerene derivatives still absorb in the near-IR region where C_{60} no longer absorbs. The extension of the linear absorption to the near-IR region is important for optical limiting applications.

OL is an optical nonlinear phenomenon which implies the increase of optical absorption as the incident radiation intensity increases. This can be obtained by different mechanisms like thermal effects, nonlinear refraction, nonlinear scattering and nonlinear absorption. Among nonlinear absorption processes, the reverse saturable absorption (RSA) is one of the most useful mechanisms. RSA is characteristic of materials with excited states absorbing more strongly than the ground state. When a laser beam passes through an RSA material the absorption from the ground state allows the transfer of population to the excited states. In this way, part of the absorption occurs starting from the excited states. When the absorption cross sections (σ, the microscopic parameter related to the absorbance) of the excited states are larger than that of the ground state, the absorption increases through the RSA mechanism and the material behaves as an optical limiter. In order to know if a material can be an optical limiter it is necessary to know its photophysical parameters, like the lifetimes and the absorption cross sections of the excited states.

Excited state properties of fullerenes have been studied using picosecond and nanosecond laser-flash photolysis, by T. W. Ebbesen et al.,[8] Bensasson et al.[5,14] and Williams et al.[15] The ground state of fullerene shows a weak absorption in the whole visible range, from 300 to 700 nm, in the same region, both the singlet and triplet excited states absorb more strongly than the ground state. Particularly the triplet-to-triplet absorption spectrum of fullerene C_{60} shows a peak at around 750 nm, while fullerene derivatives exhibit a triplet absorption blue-shifted to 700 nm. These data, together with the values of the lifetimes of the excited states and the presence of a very efficient inter-system crossing, indicate that fullerenes are good OL candidates in the visible range, either through triplet absorption for nanosecond pulses or through singlet absorption for picosecond pulses.

Together with photophysical properties, the third order non-linear optical susceptibility of fullerenes has been measured by degenerate four-wave mixing (DFWM) experiments in PMMA films doped with C_{60} and C_{70} mixture (80% C_{60} and 20% C_{70})[16] and in phosphate glasses doped with C_{60}/C_{70}.[17,18] The third harmonic generation technique[19] has been used with sol–gel hybrid samples doped with a fullerene derivative. All these experiments demonstrated that both fullerenes and fullerene derivatives show good NLO responses.

The photophysical properties of fullerene can be also studied by PL spectroscopy. This is a powerful tool to investigate the properties in different configurations or in different matrices. Fullerenes in solution do not show a large fluorescence signal. A weak fluorescence has been detected at low temperature (77 K) giving a large emission with two peaks located at 620 nm, corresponding to the 0→0 transition, and at 687 nm, and a large band around 720 nm.[4] In fact, C_{60} shows characteristics of molecular semiconductors, with a highest occupied molecular orbital to lowest unoccupied molecular orbital (HOMO–LUMO) gap of about 1.9 eV, since this is a forbidden transition. Enhancement of PL properties of C_{60} is possible if the molecule is confined in a solid environment that perturbs the fullerene electronic state determining changes in the spectral selection rules and the activation of normally forbidden transitions as well as variation of the energy gap.

3. Solid matrices for embedding fullerenes

Several requirements must be satisfied to develop fullerene doped solid state materials for photonic applications, such as optical transparency, thermal and mechanical stability, high NLO activity, feasibility of films and waveguides.[20] Sometimes, these properties must be achieved simultaneously. Besides, the incorporation of organic molecules can only be made using low temperature processing, where it is possible to ensure the survival of the organic species, especially in an air atmosphere. From this point of view fullerenes show a relatively high thermal stability, but they are not soluble enough in common solvents, indispensable for the preparation of several solid materials. With fullerene derivatives it is possible to overcome the solubility problems, making the fullerene more compatible with a particular host material and to modify or even improve its optical properties. Furthermore, the materials design must allow the preparation of films, multilayers or bulks in order to make possible the design of a particular photonic device.

Notwithstanding the strict requirements on the material synthesis and properties, different materials and preparation methods have been employed to prepare fullerene doped solid state systems with good optical properties. Among them are the polymeric synthesis or the more versatile sol–gel process as well as embedding fullerenes in microporous structures, for example by impregnation methods.

The incorporation of fullerenes in polymeric matrices can be achieved simply by mixing the two components in a common solvent. A more complex synthesis, such as the polymerization in the presence of reactive fullerenes, or the copolymerization of fullerenes containing a monomer, etc..., afford chemically linked fullerenes and polymers, obtaining a larger fullerene concentration and homogeneity of the materials.[21–23] Several polymers have been chosen as the matrix for doping with C_{60} to improve utility, stability, processability and optical nonlinearity of C_{60}. This has been done in order to obtain optical quality guest–host structures and easy film processability.

By using chemical processes, the sol–gel method allows us to produce ceramic materials, in particular high optical quality glasses, hybrids and aerogels.[24,25] These matrices are suitable to be used as a host for optically active species at relatively low processing temperatures, compared to a traditional melting and sintering process, especially in the case of hybrid sol–gel glasses.[26–28] These materials can be prepared by many complex chemical processes allowing a large engineering of the ceramic microstructure on a nanometric scale, that also possesses the important property of withstanding high-energy laser pulses. To increase the inclusion of fullerenes in sol–gel matrices, a large number of studies have been conducted to functionalize pristine fullerene and produce fullerene derivatives suitable for the sol gel process.[29–34] The main properties of these derivatives are large solubility in organic solvents, very poor in the pristine fullerene, and the presence of reactive groups, that may chemically link fullerene to the sol–gel network during the materials

synthesis.[35] These properties decrease its tendency to aggregate and to form clusters during solvent evaporation and allow higher quality sol–gel materials with high fullerene concentrations to be obtained.[36] Doping by diffusion or impregnation processes can be an alternative solution to embed fullerene in porous inorganic solid matrices synthesized at high temperatures, but the achievable fullerene concentration is generally limited.

Incorporation of fullerenes in porous materials either by impregnation and diffusion methods or during the synthesis process is an important and promising issue because it allows strong fullerene constraints in order to promote confinement effects. This confinement preserves the molecular (or small aggregates) state of fullerene and the interactions with the wall pores give rise to a perturbation of the delocalized π orbitals which in turn cause the optical properties of the fullerene.

The choice of a specific processing method is strictly related to the doping material and the desired optical properties. In some cases it is interesting to generate interactions between the dye (guest) and the matrix (host), each being able to enhance the optical properties of the other. On the other hand, for different purposes, it is desirable to obtain a good guest dispersion without strong interactions with the host materials. The optical properties obtained can be deeply different.

4. NLO properties dependent on strong interactions between the host dye and the matrix

A material, with high nonlinear optical susceptibility, has potential applications in optical devices. A possible way to improve the nonlinear optical response is the modification of the electronic structure of the material. For organic molecules, like fullerenes, the donor–acceptor structure has been widely used to get improved second- and third-order nonlinear optical response. The intramolecular charge transfer (CT), from the donor polyenic chains of polymers, to the acceptor fullerene, enhances the nonlinear optical response of C_{60}. CT is a fast process, occurring within 300 fs after photoexcitation, since it is more than 100 times faster than any competing process, the process presents an almost unitary yield.[37]

Several polymers have been chosen to obtain charge transfer complexes formed by fullerenes and polymeric matrices. In fact, it has been demonstrated, by Lascola *et al.*, by the use of coherent anti-Stokes Raman Spectroscopy (CARS), that the value of the second order hyperpolarizability of charged species C_{60}^- is more than 65 times greater than the corresponding value of neutral species. The possibility of reaching the total charge separation during the CT process would increase the nonlinear optical response of fullerene.[38]

Interactions of fullerenes with the matrices modify their electronic structure and also lead to strong luminescence. This can be done by embedding C_{60} in microporous structures having pores of 1.5 nm diameter. Trapping in microporous solids with a larger channel diameter also produces great enhancement of light emission and a blue shift of photon energy with respect to pristine fullerene, due to a quantum confinement effect (QCE) of the molecules or small clusters. Therefore, the selection of the matrix is important to change the property of C_{60} light emission.

In the following, a few examples of the improvement of the ultrafast NLO properties of fullerene doped polymers and PL features of fullerene confined in different matrices are described.

4.1 Fullerene third order nonlinearity in charge transfer complexes

When the inclusion of C_{60} in polymeric matrices allows the formation of charge transfer complexes, the nonlinear optical responses are enhanced. Gong *et al.* reported results of

polytetrahydrofurfuryl methacrylate (PTHFMA) doped with C_{60}.[39] Fullerene acts as electron acceptor, while the oxygen atoms of the polymer shows a donating nature, they form together a charge transfer complex in C_{60}–PTHFMA copolymers. High optical quality films have been prepared by casting a benzene–chloroform mixed solution in which both PTHFMA and C_{60} were dissolved. After evaporation at room temperature 0.2 mm thick films were obtained with a C_{60} content of about $2 \div 5 \times 10^{-4}$ M. The optical properties of these samples have been measured through the ultrafast optical Kerr effect (OKE) technique at 640 and 820 nm. The intensity of the OKE signal is proportional to the third order optical susceptibility, $\chi^{(3)}$. Experimental data of the C_{60}–PTHF complex, at 640 nm, have been compared with those of pure C_{60}, showing that the complex possesses a larger (enhanced by about one order of magnitude) third order optical susceptibility. Since no OKE has been found at 820 nm, it has been assumed that the large third-order nonlinearity for the charge transfer complex was related to the two-photon resonance.

The improvement of NLO susceptibility has also been achieved by Ma *et al.* with a new synthesized star-like $C_{60}(CH_3)_x$-$(PAN)_x$ copolymer.[40,41] This compound presents the fullerene cage at the center, with several PAN chains and -CH_3 groups linked. Films, 1 µm thick, have been prepared by a physical jet deposition technique on silica substrates at 350 °C. The presence of an intramolecular CT effect, due to the link of the PAN chain with the fullerene cage, has been observed from the absorption spectra. The copolymer films show new absorption peaks in the near ultraviolet (UV) region, from 335 to 370 nm, related to the intramolecular CT excited state. The comparison of PL and excitation spectra of pure PAN and the star-like copolymer indicates a partial quenching effect in the copolymer, reflecting the excitation transfer from the PAN chain to the central fullerene. The improvement of the ultrafast nonlinear optical response has been demonstrated through OKE measurements, by comparing the OKE signal of the copolymer to the OKE signal of CS_2. The real part of the third-order nonlinear optical susceptibility of the copolymers, calculated from the OKE signal, is related to the PAN concentration within the copolymer: with high PAN concentration the optical susceptibility is four times larger than that of the pure polymer.

4.2 Optical limiting of fullerene containing donor–acceptor systems

Solid systems have been properly designed to allow the CT processes and enhance the OL of fullerenes. Cha *et al.* reported NLO absorption of solid films of poly(3-octylthiophene) (P3OT) sensitized with methanofullerene, in the range from 620 to 960 nm.[42] The photoinduced intermolecular CT enhances the nonlinear absorption by more than two orders of magnitude. The generated charge excited states show large absorption, thus the system seems to be promising for OL purposes. A fullerene derivative, the phenyl-C_{61}-butyric acid cholesteryl ester, denoted as (6,6)PCBCR, and pure P3OT, dissolved in xylene have been mixed with a 1 : 1 mixture. The filtered solutions were cast onto fused silica substrates, in order to obtain thick films (20–30 µm) or prepared by spin coating, to obtain thin films (0.1–0.2 µm). The effective two-photon absorption (TPA) coefficients (β_{eff}) have been measured by open aperture z-scan experiments. It has been shown that, at 760 nm, the β_{eff} of the composite film is enhanced by more than two orders of magnitude with respect to a pure film of P3OT or a pure film of (6,6)PCBCR. This large enhancement is believed to arise from charge transferred states. Open aperture z-scan data have also been fitted with an appropriate model, which takes into account the excited state population generated. These data, compared with picosecond photoinduced absorption spectra, confirm the presence of the CT mechanism. The large nonlinearity, found at 760 nm, can be employed for OL

purposes. P3OT/(6,6)PCBCR films, 30 μm thick, with T_{lin} = 0.44, at 760 nm, show good OL: the output fluence is 0.1 J cm^{-2} at an input fluence of 1 J cm^{-2} and the damage threshold is around 1 J cm^{-2}.

OL measurements in systems where donor–acceptor interaction reinforcement is present were also studied by Kamanina et al.[43,44] In ref. 44, polyimide thin films doped with fullerene are considered for their OL effect in the IR spectral range. Fullerene doped polyimide films of 2–3 μm were prepared by spin coating a 1,1,2,2-tetrachloroethane 5–6.5% 6B and 81A polyimide solution containing 0.1–1 wt% of C$_{60}$ or C$_{70}$. The dependence of the transmission as a function of the input energy was measured at 1315 nm with a photodissociation iodine laser; the low-power transmission of photosensitive 6B and non-photosensitive 81A polyimides are about 0.85 and 0.75 respectively. By comparing the output *versus* input energy density plots of polyimide 6B films with 0.2 and 0.5 wt% of C$_{70}$, differences in the transmission ascribed not only to the different concentrations were found: a drastic attenuation of the laser energy density of a factor 9–12 with 0.5 wt% at 0.8 J cm^{-2} (with 0.2 wt% the attenuation was about 3 at the same energy density) was attributed to the activation of a complex formed between a donor fragment (triphenylamine) of the polyimide molecule and fullerene. In these conditions, the RSA material based on polyimides has an absorption cross section of the donor(polyimide 6B fragment)–acceptor(fullerene) complex about 300 times larger than the one of the intramolecular polyimide complexes.[45]

The OL of fullerene containing polyimides has been investigated and theoretically analyzed with different samples.[46,47] Thin films, 1 μm thick, have been prepared by spinning on glass substrates, 1,1,2,2-tetrachloroethane (TCE) solutions of polyimide, malachite green dye and fullerenes (a mixture of C$_{60}$ and C$_{70}$). The OL measurements, at 532 nm, show that the best performances have been reached with samples doped with fullerenes and malachite green dye simultaneously. By comparing the OL curves of samples doped with 0.5 wt% of fullerenes, with and without malachite green dye, it is possible to observe that the OL performances increase, more than 6 times when malachite is present. The attenuation observed has been estimated to be 10–15 times for the fullerene–dye–polyimide system, while, with fullerene–polyimide and dye–polyimide, it was 2–3 and 4–8 times respectively. The presence, at the same time, of fullerenes and the dye allows the formation of CT complexes, as it has been described theoretically with the Förster model.

OL in polystyrene doped C$_{60}$ solid films has been observed by Kojima et al., who synthesized the polystyrene-bound C$_{60}$ by reaction of styrene in the presence of C$_{60}$ under high pressure.[48] Optical measurements have been performed on a 1 mm thick solid sample (with 0.2 wt% of C$_{60}$), made from reacted solution under pressure (0.1 GPa, 200 °C 5 h) and on a C$_{60}$ styrene solution. Authors found a decrease of the linear transmittance from 55% to 20% after the reaction and an OL effect about 5 times grater in the solid sample than in the corresponding solution. This fact has been explained by suggesting an increased excited state absorption cross section of C$_{60}$ by binding with polystyrene or a blue-shift of the triplet-to-triplet absorption peak.

4.3 Effect of the fullerene molecule–matrix interaction on PL properties

The sponge-like structure of porous silicon (PS) with a pore size of about 1.5 nm allows the trapping of C$_{60}$ molecules and leads to strong interactions between C$_{60}$ molecules and Si surface pores.

C$_{60}$ molecules have been embedded in porous Si by different methods: physical deposition, chemical coupling[49] or C$_{60}$ implantation.[50] An intense and well resolved photoluminescence has

been revealed with a large number of fine-structure peaks, assigned to vibrational progression coupling with electronic states of C$_{60}$ induced by the interaction between the molecule and the surrounding silicon surface.[50] Moreover, it has been shown that C$_{60}$ can emit PL comparable with the PL signal from porous silicon even at room temperature.[49] Beside the peak at 730 nm correlated with perfect C$_{60}$, two new peaks were revealed, one at 620 nm, associated with C$_{60}$ molecules adsorbed in the Si pores, and a peak at 630 nm, associated with the molecules coupled to the porous Si. The PL enhancement has been explained by the contribution from porous Si, that acts as a carrier generator and by the embedded C$_{60}$ molecules which work as radiative recombination centers. The carrier transfer between porous Si and C$_{60}$ molecules is thus playing the main important role in the enhancement of fullerene PL.

PL from mesoporous silica molecular sieves containing C$_{60}$ has been reported. The intensity of the PL signal data suggests that C$_{60}$ has been confined in the sieve channels and that host and guest may interact with one another.[51]

Enhanced PL at room temperature has been reported for C$_{60}$ molecules confined in zeolites, porous crystalline aluminosilicates with an open molecular cage structure characterized by a controlled pore size of about 0.4–1.8 nm, similar to the dimensions of many organic molecules. C$_{60}$ is incorporated in the zeolites by vacuum or vapor transport methods[52–54] or from benzene solution at high pressure.[55–57] Also in this case intensive PL response is observed, by revealing intense white light emission,[55] or emissions in different regions[52,53] from confined C$_{60}$ molecules. The strong perturbation of their molecular orbitals is probably caused by the interaction with the pore wall; in fact, the polar environment determines a strong polarization of the molecule that can be revealed by a UV-Vis absorption spectra shift.

A different example of fullerene doped matrices which exhibit stronger PL with respect to their undoped counterparts has been prepared by Wang et al.[58] The following matrices have been tested: nano-ZrO$_2$, nano-Al$_2$O$_3$, nano-SnO$_2$, and polystyrene. The nanooxides were prepared by immersing the activated oxide powders in a C$_{60}$ saturated solution and pressing the dried powders, while the polystyrene was dissolved with C$_{60}$ in toluene. X-Ray diffraction (XRD) spectra showed that C$_{60}$ is dispersed, as single molecules, in all these matrices. PL data are similar: a wide luminescence band from the visible to the near-infrared region, with intensities 3 to 10 times stronger than the undoped matrix and the peak between 585 and 610 nm. This fact confirms that the PL signal originates from fullerene transitions. It has been suggested that the blue shift, observed in the PL signal compared with that in powders, derives from C$_{60}^+$ or C$_{60}^{n+}$ species formed in the matrices due to the presence of CT interactions between the C$_{60}$ molecules and the matrix. A different mechanism to enhance photoluminescence was studied by Zhang et al. in doped polystyrene.[59] Under simultaneously exposure to UV-Vis light and oxygen, C$_{60}$ undergoes a photoassisted reaction with molecular oxygen. The presence of O$_2$ suppresses the formation of the C$_{60}$ polymer, otherwise observed, and the sample exhibits a fluorescence spectrum blue shifted and with an intensity increased more than 10 times with respect to the fresh non-irradiated sample.

C$_{60}$ has also been incorporated into phosphate and fluorophosphate optical glasses obtained by the melting procedure.[60–62] The chemical bonds and tight confinement strongly deformed the fullerene molecules and distorted the molecular symmetry of fullerene; these effects cause remarkable changes to the fluorescence spectrum. In particular a broad PL should be caused by amorphous islands of microstructures related to fullerene complexes (fullerene molecules bonded with [PO$_4$]$^-$ tetrahedra). An enhancement of the PL intensity and a remarkable narrowing of PL width suggested that it is due to ordered microstructures of the fullerene complex. Scanning μ-PL measurements showed

that amorphous microislands with dimensions of about 100 μm along the scanning direction are present; from these islands a strong PL and a red shift of the PL peak is observed, therefore indicating couplings between nearby fullerene complexes. Moreover, amorphous islands were found to exhibit nonlinear PL behavior. The strong confinement and chemical bonds formed with non-bridging oxygen anions may distort the molecular symmetry of fullerene leading to nonlinear dependence of PL upon laser excitation power.

5. NLO properties in matrices containing aggregates and clusters

The preparation of solid state systems in which fullerene clusters, with a typical number of molecules < 10, are confined has been reported by different authors. An increase of the PL has been observed in these materials and ascribed to the confinement effects. The formation of large fullerene cluster dimensions weakens the quantum confinement effect (QCE) and the PL features.

Some studies, aimed at determining the presence of fullerene clusters in solid matrices and investigating their effect on the material optical limiting properties, have been performed. In fact, the intersystem crossing efficiency to the triplet state is strongly worsened if C_{60} aggregates are formed and several studies have been devoted to the comprehension and explanation of this problem, that negatively affects the OL efficiency.

5.1 Photoluminescence of fullerene clusters embedded in solid matrices

The quantum confinement effect (QCE), responsible for the photoluminescence (PL) of porous silicon, is interesting in view of preparing new types of optical-electrical materials. In fact, QCE has been considered the main reason for the increase of the emission efficiency and energy shift observed in C_{60} trapped in microporous solids with a channel diameter greater than 1 nm (a C_{60} molecule has a diameter of about 1 nm).

PL features of C_{60} in silica aerogel have been investigated by Shen et al.[63–66] by a sol–gel process, in which TEOS sols were mixed with a C_{60}–C_{70} or C_{60} toluene solution, followed by supercritical drying, silica aerogels doped with fullerene have been prepared, with concentrations of 0.001–2.5 mol% and 0.001–0.5 mol% in the case of C_{60}–C_{70} or C_{60} respectively. By mass spectroscopy and Fourier transform infrared (FT-IR) spectroscopy it has been demonstrated that the C_{60}/C_{70} molecules incorporated into silica aerogels retain the fullerene structure without forming SiO_2 complexes.[65] High-resolution transmission electron microscopy (HRTEM) together with electron diffraction revealed that within aerogels it is impossible to distinguish between fullerene and silica grains.

Photoluminescence (PL) from fullerene-doped silica aerogel samples has been measured with an Ar^+ laser, at 488 nm, as the excitation source (Fig. 1). The C_{60}–C_{70} mixture in solution shows a weak PL, with the peak located at 1.75 eV (708.5 nm), while, under similar experimental conditions, the undoped silica aerogel does not show PL. At room temperature, an intense peak has been found at around 2.26 eV (corresponding to 549 nm), strongly depending on the concentration of fullerenes: as the concentration increases the luminescence intensity decreases, the profile becomes broader and the peak shifts to the red. For low doped samples, fullerene molecules are embedded as small clusters or even individual units resulting in the QCE and consequent blue shift of the PL. The enhancement of fullerene concentration in the matrix causes the aggregation of fullerenes, forming clusters, weakening the quantum confinement effect, that is inversely proportional to the size of the "quantum dots".

In C_{60} doped aerogels, an increase and a blue shift of the PL intensity has been found after annealing under vacuum at
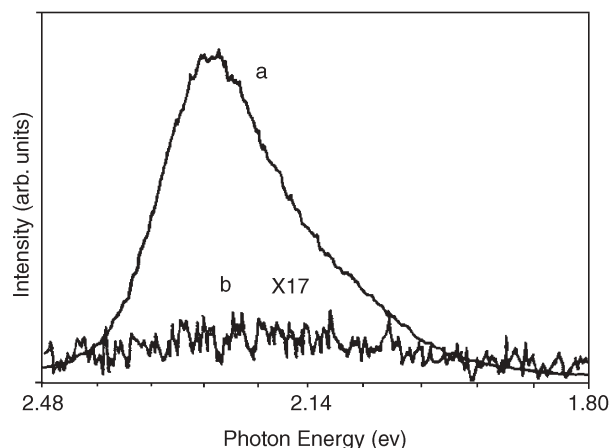

Fig. 1 PL spectra of fullerene-doped silica aerogel (0.05 mol%) (a) and of the as prepared pure silica aerogel (b) under Ar^+ excitation (488 nm, 10 mW). From ref. 65.

200 °C.[67] This has been explained by removal of residual organic molecules and adsorbed gases which could quench the light emission. The increased blue shift after annealing has been explained to be caused by the strengthening of the quantum confinement effect that follows the shrinking of the network.

Quantum size effects in C_{60}-doped sol–gel thin films has also been observed by Hasegawa et al.[68] Silica hybrid sol–gel matrices were used, based on phenyltriethoxysilane (PTEOS) and tetraethoxysilane (TEOS) in toluene and ethanol. The C_{60} toluene solution was added to the sol and a final molar ratio $C_{60}/(PTEOS + TEOS) = 0.001$ was reached in transparent films. The PL spectrum of the C_{60} doped film reveals its quantum size effects and an estimation of the cluster dimensions gave aggregates of about 10 C_{60}. The use of PTEOS was considered by the authors to be a solubilizing agent of C_{60}, rather than a silica precursor.
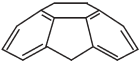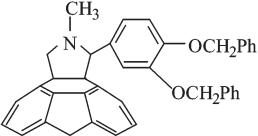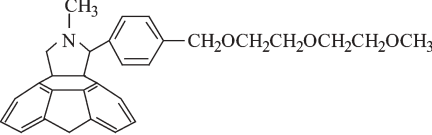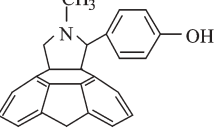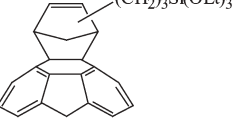
Also, larger $(C_{60})_n$ nanocrystals $(1000 < n < 10000)$ embedded in silica matrices have been prepared by vacuum deposition of silica and C_{60} nanocrystals.[69,70] PL spectra were measured at different temperatures to investigate the properties of the intermediate state between the solid and molecular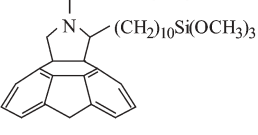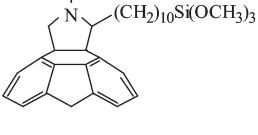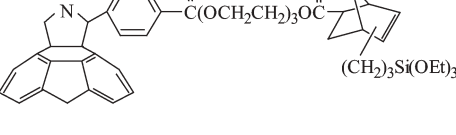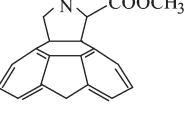 state. The PL spectra were significantly different from those of the C_{60} solid form, indicating that the vibronic coupling of the C_{60} nanocrystals in silica is strong compared with that of solid C_{60}.

5.2 Effects of C_{60} aggregates on optical limiting properties

The formation of fullerene aggregates in doped solid state matrices is an undesirable effect for optical limiting applications because the optical properties of the system are degraded. Some studies, by relaxation dynamics or photoluminescence spectroscopy, to reveal the degree of fullerene aggregation in transparent solid matrices have been made.

Amphiphilic methanofullerene derivatives have been incorporated in sol–gel matrices, showing a micellar aggregation in solution and a soaking procedure was not successful to embed methanofullerene.[71] A derivative THF–H_2O solution containing ammonia was added to the sol, that gelified in a few seconds, and the gels were dried at 40 °C. OL measurements performed on samples with a linear transmittance of 60% showed a nonlinear threshold of 2–3 mJ cm^{-2} and a damage threshold of about 100 mJ cm^{-2}. This result was explained by a large ground-state absorption cross-section $(6.5 \times 10^{-18}$ cm$^2)$ which is considerably larger than for pure C_{60} $(2.4 \times 10^{-18}$ cm$^2)$, and is probably due to the C_{60} functionalization that alters the symmetry of the molecule and decreases the forbidden character of the S_0–S_1 transition.

Table 1 Fullerene derivatives used in the synthesis of sol–gel materials for OL applications and their solubility in THF

Fullerene derivatives	Ref.		Solubility (THF mg mL^{-1})
[structure: C$_{60}$ fullerene derivative]	75,77	**C$_{60}$**	≈0
[structure: fulleropyrrolidine, CH$_3$–N, aryl with OCH$_2$Ph, OCH$_2$Ph]	30,75,76	**1**	1.2
[structure: fulleropyrrolidine, CH$_3$–N, aryl–CH$_2$OCH$_2$CH$_2$OCH$_2$CH$_2$OCH$_3$]	76,121	**2**	31
[structure: fulleropyrrolidine, CH$_3$–N, aryl–OH]	30,76,77,121	**3**	1.0
[structure: fullerene with (CH$_2$)$_3$Si(OEt)$_3$]	29,78	**4**	27
[structure: fulleropyrrolidine, (CH$_2$CH$_2$O)$_3$CH$_3$, N–(CH$_2$)$_{10}$Si(OCH$_3$)$_3$]	29,121	**5**	216
[structure: fulleropyrrolidine, CH$_3$–N–(CH$_2$)$_{10}$Si(OCH$_3$)$_3$]	29,121	**6**	27
[structure: fulleropyrrolidine, CH$_3$–N, aryl–C(O)(OCH$_2$CH$_2$)$_3$OC(O)–norbornene–(CH$_2$)$_3$Si(OEt)$_3$]	29,121	**7**	61
[structure: fulleropyrrolidine, (CH$_2$)$_3$Si(OEt)$_3$–N, COOCH$_3$]	29,74,81–85,102,121	**8**	43

Time resolved pump-probe experiments indicate the presence of a fast relaxation from the singlet excited state which can be attributed to interactions between the fullerene spheres of neighboring molecules in clusters. This relaxation affects the OL behavior of the sol–gel samples against ns laser pulses.[72]

Negative consequences on OL performances attributed to interactions between the fullerene cages were also noticed in the early works of the University of Padova group.[29] Sol–gel hybrid materials based on methyltriethoxysilane (MTES) and doped with different fulleropyrrolidines[29–34,73–76] (FP in Table 1) have been prepared.[77–79] The derivatives reported in Table 1 have different solubilities, depending on the particular functionalization, and in some cases (derivatives **3–8**) can lead to chemical bonds with a sol–gel matrix. The OL measurements

have been performed with 15 ns pulses from an excimer pumped dye laser, emitting at 532 and 652 nm, and the transmitted radiation has been collected by a detector, with an acceptance angle of about 1×10^{-2} srad. The experimental data show large differences in the OL performances of hybrid matrix solid samples with respect to those measured in solution. This has been only partially justified by the lower contribution of nonlinear scattering in solid samples than in solution, as it was observed by other authors and herein described later (Section 6.2).[80] Moreover, OL measurements taken from different spots of the same sample have given different OL efficiency: larger efficiency values have been obtained even when high transmittances, larger than those expected from Lambert–Beer's law, were measured. These observations suggested that linear scattering effects are present in these doped MTES based matrices, despite a fullerene derivative that may covalently link to the silica network being used. In fact, the formation of fullerene clusters probably occurs during the densification process and can hardly be controlled in this sol–gel procedure. This, together with a certain degree of porosity, determines the presence of structural inhomogeneities that were mainly found in the thicker sol–gel slabs, where larger linear scattering effects were observed. In these samples the decreasing of OL efficiency is thus ascribed to the apparent decrease in linear transmittance measured by limited aperture detection.

The OL performances of different derivatives in MTES based matrices have been reported in Table 2. The figures of merit (FOM) have been calculated by the ratio between the linear transmittance and the nonlinear transmittance at the maximum input fluence reached or at the damage threshold. It is possible to observe that the choice of an appropriate FP is very important to obtain higher performances, as evidenced, for example, by comparing the behaviour of derivative **6** with **3** in Table 1.

Moreover, further improvement of optical quality of sol–gel glasses has been shown to be possible by using particularly promising hybrid sol–gel systems, which allow formation of the gel phase without using a high treatment temperature normally necessary to eliminate the final sol–gel porosity.

The group at University of Padova have obtained an improvement of optical quality of sol–gel matrices with hybrids based on 3-(glycidoxypropyl)trimethoxysilane (GPTMS). These matrices allowed more dense materials to be obtained without using the high treatment temperature normally necessary to eliminate the final sol–gel glass porosity ($T \approx 100\ ^\circ\mathrm{C}$); moreover, they were found to dissolve larger fulleropyrrolidine amounts (up to 4×10^{-2} **8** l^{-1}). Despite this, large linear scattering effects were not observed in these FP doped systems, clustering effects on a lower scale were in any case found depending on the synthesis procedure and on the resulting hybrid glass microstructure.

The effect of different matrix microstructures on the OL of FP has been investigated with regard to fullerene aggregation and the following OL efficiency degradation. Refs. 81–83 report the investigation of the microstructure effect of similar hybrid matrices incorporating the *N*-[3-(triethoxysilyl)propyl]-2-carbomethoxy-3,4-fulleropyrrolidine (the fulleropyrrolidine **8**, in Table 1), hereafter denoted as FULP.

Hybrid matrices have been prepared from 3-glycidoxypropyltrimethoxysilane (GPTMS). Different Lewis acids have been used as epoxy ring polymerisation agents, $\mathrm{Zr(OBu^t)_4}$, $\mathrm{BF_3}$, $\mathrm{SiCl_4}$, $\mathrm{Ti(OBu^t)_4}$, $\mathrm{TiCl_4}$, $\mathrm{Ti(OPr^t)_4}$, that also behave as inorganic oxide network formers. FULP molecules were dissolved in tetrahydrofuran and then added to the different sols. The concentration of FULP in these matrices is about 3×10^{-3} FULP l^{-1}. Different degrees of organic polymerisation are obtained by changing the Lewis acid because the competition between the inorganic and organic polymerisation changes the microstructure properties of the matrix. A correlation between the two aspects was found because a higher degree of organic polymerisation determines an enhancement of the FP dispersion in the sol–gel matrix.[81] Moreover, by comparing $\mathrm{SiO_2}$–$\mathrm{TiO_2}$ hybrid matrices, based on GPTMS and obtained with different synthetic procedures, it has been observed that FP clustering is present when the formation of a larger $\mathrm{TiO_2}$ cluster size in the inorganic network, revealed by UV-Vis spectra, occurs. This gives rise to a less homogeneous heterometallic network.[84,85] Notwithstanding, all the $\mathrm{SiO_2}$ and $\mathrm{TiO_2}$ samples appear transparent, an evident consequence is revealed in the OL efficiency as well as in the laser damage threshold: both decrease with increasing $\mathrm{TiO_2}$ cluster size.

6. NLO properties of isolated fullerene molecules in solid state matrices

Weak interactions between the fullerene cage and the surrounding matrix always exist, several examples of NLO properties of fullerene embedded in solid matrices that can be ascribed to the isolated molecule have been reported, in which any weak interaction with the solid medium can be reasonably disregarded. In this respect, mainly OL applications were investigated and fullerene properties were often found to be similar to those of solution dispersion, as many studies have confirmed. Only a few studies on OL applications revealed the presence of weak fullerene–matrix interactions that negatively affect the quantum yield of intersystem crossing and determine evident PL.[86,87] However, in these cases, the interactions are weak enough to give a sufficiently large triplet state lifetime and OL features are still observed.

It is important to underline that an improvement of the sol–gel doped glass and polymeric matrix quality and an increase of the fullerene concentration in the final matrix can be obtained by using fullerene derivatives instead of pristine fullerene. This has been experimentally verified and reported by several research groups. Besides the enhanced solubility in a suitable solvent for sol–gel processes, the presence of reactive groups that covalently link the derivatives to the inorganic network allows optimization of the sol–gel procedure. Transparent films or bulk samples can be prepared, without evidence of fullerene cluster formation and good OL properties.

6.1 OL of fullerene doped polymeric matrices

Fullerenes have been incorporated in several types of organic polymers: poly(methyl methacrylate) (PMMA),[80,88] bicyanovinylpyridine,[89] and polysilanes.[90]

The first OL measurements on polymeric matrices were performed by Kost *et al.*, with $\mathrm{C_{60}}$ in PMMA samples.[80] To prepare thick bulk samples, with a thickness of about 7.1 mm, PMMA and $\mathrm{C_{60}}$ have been dissolved in a solvent, that was then removed from cast films, by heating and evacuation steps. The sample is pressed (14–21 MPa) in a preheated die ($T \approx 160\ ^\circ\mathrm{C}$); thinner films (1.7 and 4.9 mm) have been cut from it. The $\mathrm{C_{60}}$ concentration in PMMA was 0.06% by weight and the linear transmittance of a 1.7 mm thick sample was 69%. The $\mathrm{C_{60}}$ OL in PMMA has been compared with that in toluene and with PMMA samples containing different OL molecules, like chloroaluminium phtalocyanine (CAP), *N*-methylthioacridone, King's

Table 2 OL properties of sol–gel hybrid matrices based on MTES

$\mathrm{C_{60}}$-FP	Concentration/M	T_{lin} %	FOM (T_{lin}/T_{NL}) 532 nm	Ref.
$\mathrm{C_{60}}$	1.2×10^{-3}	68	1.31	121
3	1.1×10^{-3}	38	1.65	29,121
3	2.3×10^{-3}	27	1.48	29,121
4	2.3×10^{-3}	70	1.59	29,121
6	2.3×10^{-3}	30	3.3	29,121

complex $[(C_5H_5)Fe(CO)]_4$, and ruthenium King's complex $[(C_5H_5)Ru(CO)]_4$. OL, at 532 nm with 8 ns pulses, has been observed in C_{60}–PMMA samples, with different thickness, and compared with OL calculated curves, based on the RSA model. Good agreement between the experimental and the calculated data confirmed that C_{60} OL in PMMA is due to excited state absorption. By comparing OL behavior of C_{60} in solution and in a solid sample, it has been observed that the first one shows higher OL, by a factor of about 2. This has been attributed to the presence in C_{60} solutions of nonlinear scattering, contributing, at higher fluences, to the total OL. The damage threshold of C_{60} PMMA samples has been in the range 1.2 and 1.8 J cm^{-2}. The comparison with different OL molecules in PMMA showed that only CAP and N-methylthioacridone possess comparable OL, at 532 nm, but only C_{60} can be a broad band optical limiter, since it possesses an excited state absorption cross section larger than the ground one in a larger visible range. Time resolved techniques, with ns and ps pulses, have also been used to observe transient OL processes in C_{60} in PMMA matrices and to compare with theoretical models. The results confirm the presence of good OL, at 532 nm, with ns pulses, characterized by a fast "switching speed" of the optical power limiter, less than 5 ns.[91]

A different mechanism, explaining the differences in OL performances of C_{60} in solution and in PMMA, has been proposed by Riggs and Sun.[92,93] They investigated the OL behavior of tert-butyl methano-C_{60} carboxylate in PMMA, in highly viscous media and in toluene solutions and compared it with chloroaluminum phthalocyanine (Cl-Al PC) behavior, under the same conditions. Their starting point is the consideration that the OL behavior of C_{60} in solution at 532 nm is strongly dependent on fullerene concentrations. By observing the OL of solutions, with differences of 2 orders of magnitude, they supposed the presence of bimolecular excited-state processes, diffusional or pseudodiffusional in nature, contributing in concentrated samples to the total OL. Besides, the medium viscosity significantly influences the OL performances of C_{60}. Measurements were performed on solutions, toluene–PMMA polymer blends, thin and thick PMMA films, all containing methano-C_{60} derivatives. While the absorption spectrum of the methano-C_{60} derivative in a toluene–PMMA polymer blend is not different from the spectrum in solution, the OL response exhibits weaker responses in the highly viscous medium, measured in a 2 mm thick cuvette having a linear transmittance of 71%. A similar result was obtained if a doped poly(propionylethyleneimine) polymer blend was used instead of PMMA blend, ruling out the possibility that specific interactions between the methano-C_{60} derivative and PMMA exist. Finally, OL in PMMA methano-C_{60} doped films with different thicknesses (0.1–0.4 mm), made by spin-casting on silicon or glass substrates from derivative solutions in a toluene–polymer blend, were performed and compared with solution samples with similar linear transmittance. It has been shown that the OL of solid PMMA samples are independent from the film thickness, by comparing the nonlinear behavior of samples with a linear transmittance of 80% and different thicknesses. Moreover the OL of the PMMA sample is different from solutions with the same linear transmittance, confirming once again that RSA is the prevalent contribution to the OL.

Procedures that covalently link fullerene to the polymer chains were developed for PMMA[94] and polystyrene,[95–97] but only a few OL experiments in solid samples have been performed until now. These procedures would allow a higher concentration and homogeneous dispersion of the fullerene in the polymeric matrix, with respect to pure dispersed C_{60}. The attempts made with benzylaminofullerene (BZAF) to form copolymers, showed that this new compound still works well in solution, but lower performances, limiting thresholds one order of magnitude less, are obtained in solid copolymer samples.[94]

6.2 OL in sol–gel matrices

Different studies have been done on sol–gel matrices showing evidence of small interactions that influence the properties of the embedded fullerenes.

C_{60} embedded in solid mesoporous matrices, have been prepared with tetramethoxysilane (TMOS):[72,98,99] TMOS was hydrolyzed in acidic conditions with formamide and the gel was treated at 500 °C. The resulting mesoporous material (mean pore diameter of 3.7 nm) was doped with C_{60} by soaking the glass with a saturated chlorobenzene C_{60} solution giving a good dispersion of the molecules.

C_{60} doped samples with 50–60% linear transmittance, have been investigated through pump-probe experiments, at 532 nm, with 32 ps pulses. The dynamic studies show that the first increase of population is due to population of the first excited state. The following exponential decay leads to a plateau, on a nanosecond time scale, indicating the presence of the inter-system crossing process, having an unitary yield and with a time constant of 150 ps. This time is slightly shorter than 1000 ps measured in C_{60} chlorobenzene solutions, clear evidence of the presence of interactions between the C_{60} molecules embedded in the pores of the matrix. Moreover, although the triplet quantum yield is reduced when compared to aromatic solvents, it is still 25% i.e. not negligible as in the case of crystalline C_{60} films (Fig. 2).

OL measurements, at 532 nm with 32 ps pulses, show a nonlinear threshold of about 10 mJ cm^{-2} and a damage threshold between 1 and 2 J cm^{-2}, even if a cumulative damage was revealed after 200 mJ cm^{-2} for repetitive pulses and bleaching effects can be observed with OL measurements. In fact, at
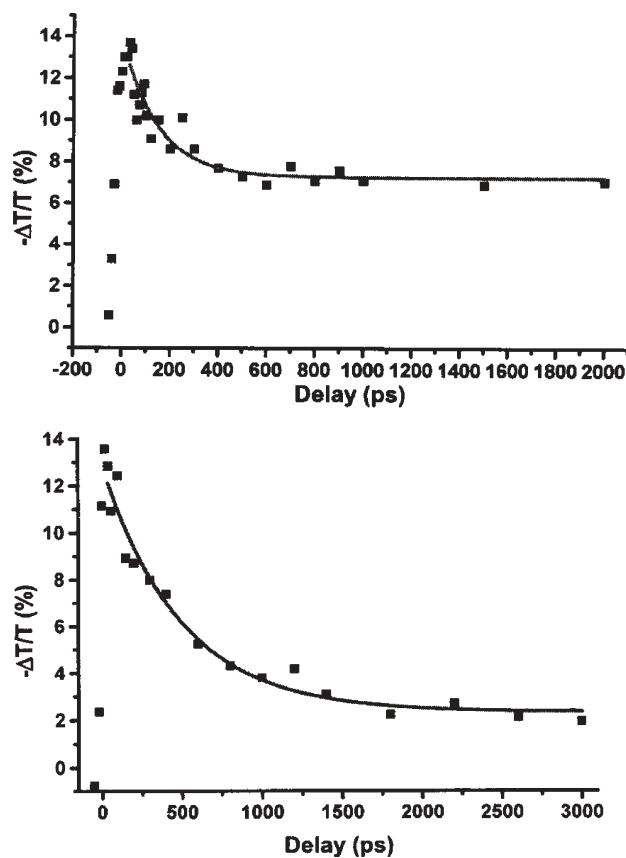

Fig. 2 De-excitation dynamics of the S1-level for sol–gel glasses impregnated by pure C_{60} (top) or doped with methanofullerene, measured by degenerate pump-probe experiments. In the second case the existence of a long lived triplet state is still evident but the triplet state-induced absorption is less pronounced than for pure C_{60}, a consequence of the aggregation. From ref 72.

input energy larger than 200 mJ cm^{-2}, the transmittance of the sample at input energy gave fixed increases as a function of the number of laser shots.

The comparison of C_{60} experimental and theoretical behavior in solution and in xerogel samples, previously described, indicates that both singlet and triplet excited states saturate in solid samples for high fluences.[86,99] On the contrary, in solution it is not possible to see the saturation due to the presence of different mechanisms, like thermal effects or bubble formation. The analysis of the transmission changes during double pulse pump probe experiments and the resulting population distribution confirm that in xerogel glasses the dynamics are faster than in solution. On a ns time scale, the triplet excited state population of C_{60} in solution increases linearly, with a quantum yield of 0.85, while in solid samples a saturation is reached and the triplet quantum yield of the inter-system crossing effect is around 0.25, *i.e.* not negligible as in the case of crystalline C_{60} films. The lifetime of the triplet excited state is shorter than in solution, but still long enough to allow efficient OL on a ns time scale. The authors explain the differences in triplet yield and the faster dynamics in the solid matrices, if compared to solutions, by the absence of an aromatic solvent, that stabilizes C_{60} excited states, and by the perturbation of the molecular energy levels deriving from the interaction with the solid environment.

Other OL experiments in sol–gel matrices doped with fullerenes have been performed by G. Fuxi *et al.*, who doped SiO_2 and SiO_2–TiO_2 (Si : Ti = 8 : 2) inorganic gels with 0.3 wt% of C_{60} or C_{70}. A 1-methylnaphtalene (bp = 243 °C) solution of fullerene was dissolved in the sol and the resulting dried gel was heat treated at 140 °C for two weeks.[87] The addition of a small amount of *O*-dimethyl phthalate into the sol was found to improve the formation of transparent and uniform gels. An inhomogeneous broadening of the absorption spectra of fullerene in sol–gel samples compared with those in solution was observed and ascribed to the interaction of fullerene molecules with the matrix and confirmed by strong fluorescence intensities. OL measurements at 532 nm confirmed the limiting behavior of the SiO_2 doped glasses.

Generally speaking, RSA and photoinduced scattering are the main contributing processes to the OL effects. For fullerene containing solid state materials RSA plays the dominant role, because the small-scale inhomogeneity produced by light incidence cannot evolve during irradiation. Belusova *et al.* showed the absence of nonlinear scattering to the OL in C_{60} and C_{70} doped sol–gel, microporous SiO_2 and polymeric matrices and compared the results with fullerene solutions, where essential contribution to the attenuation was made by photoinduced processes connected with small-scale changes in refractive index.[100,101]

An in-depth study of the OL behavior of fullerene containing sol–gel materials and solutions has been made by Signorini *et al.*[102,103] By these studies it turns out that the optical properties do not change substantially in going from the solution to the sol–gel. Hybrid sol–gel samples, based on GPTMS, tetraethoxysilane and $Zr(OBu^t)_4$ (named GPTMS-Zr), have been doped with FULP (compound **8**) and the linear and nonlinear optical properties of bulk samples have been compared with those in solutions. The results of the linear absorption spectra are reported in Fig. 3, while Fig. 4 reports the OL behavior of a 1 mm thick bulk sample compared with a 10 mm FULP solution in toluene, with similar linear transmittance, of 0.80 and 0.74 respectively.

From Fig. 3 it is clearly shown that the linear absorption spectrum of FULP in sol–gel overlaps that in solution. The comparison of OL measurements of FULP solutions with those of sol–gel samples having a similar linear transmittance do not differ appreciably. These data clearly confirm that the inclusion of FULP in a hybrid GPTMS-Zr sol–gel matrix do not affect the optical properties of FULP. With these solid
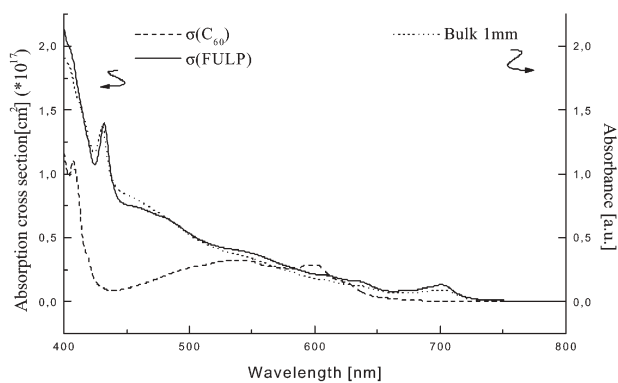
Fig. 3 Linear absorption spectra of **8** (solid line) and C_{60} (dashed line) solutions in toluene (10 mm thick) and derivative **8** doped 1 mm thick sol–gel sample (dotted line). From ref. 102.

samples a molecular dispersion similar to that of solutions has been reached.[102] This fact, confirms that, if properly designed, sol–gel doped materials allow a uniform dispersion of the fullerene molecule in transparent solid media, without any other effect on the desired optical properties.

The similarity of the nonlinear behavior in bulk and in solution allows also ascribing the origin of the nonlinear absorption to the RSA mechanism. The OL of FULP in solution has been attributed principally to the RSA mechanism, by comparing the experimental data with calculated curves[103–106] The last ones are based on the RSA model, which considers the space- and time-evolution of the energy level populations entering the NL processes, by solving a system of coupled kinetic equations. Using the RSA model it has been shown that in solution the RSA mechanism is the principal contribution, while nonlinear scattering and nonlinear refraction occur at higher fluences. Since FULP in solution and in a sol–gel matrix show the same behavior the principal origin of the nonlinear absorption in sol–gel has also been attributed to the RSA mechanism.

This fact has also been experimentally confirmed by open- and closed-aperture OL measurements.[102,103] It is possible to separate the NL scattering contribution to the OL by comparing OL measurements made with a large acceptance angle (open-aperture) at the detector with those made with a small angle (closed-aperture). In the first case the NL scattering does not contribute to the OL while in the second case it does. The contributions of NL scattering to the OL of doped sol–gel samples with different thickness and linear transmittance (0.5, 1.0 and 1.4 mm, T_{lin} = 0.86, 0.76 and 0.52 respectively) have

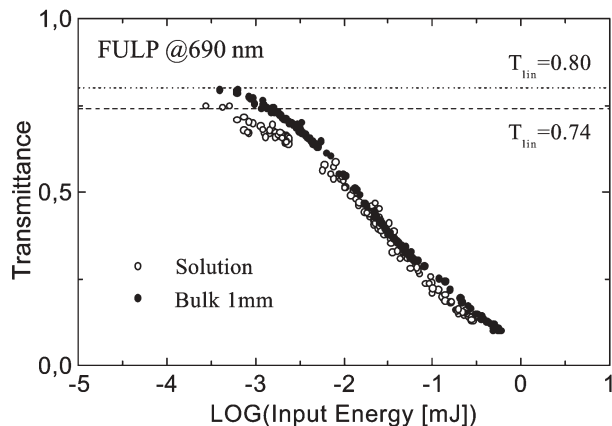**Fig. 4** OL data at 690 nm of FULP toluene solution, with T_{lin} = 0.74 and 1 mm FULP doped GTZ sol–gel matrix, with T_{lin} = 0.80 (from ref. 103).
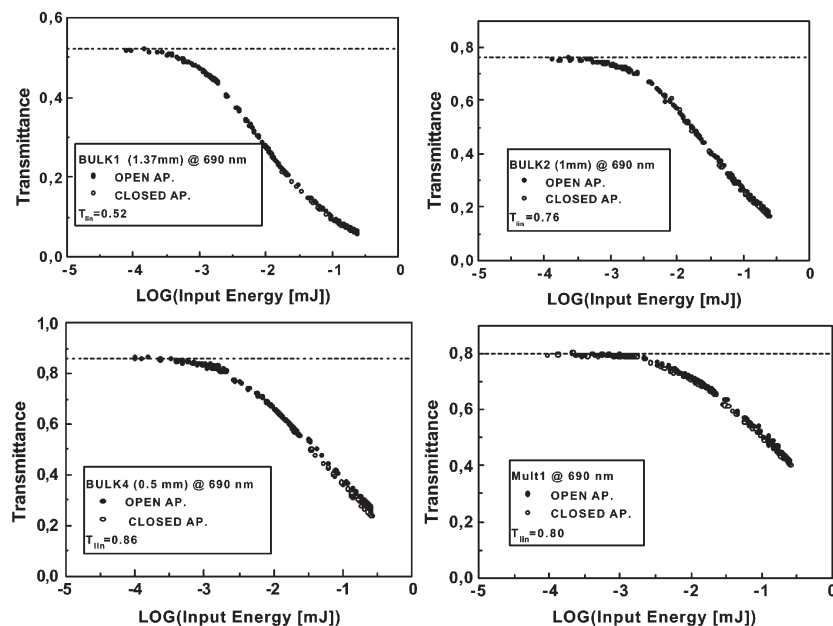
Fig. 5 Open (full circles) and closed (open circles) aperture experimental OL data of FULP doped sol–gel samples at 690 nm (from ref. 103).

been measured at 690 nm; unlike the solutions, they do not show appreciable NL scattering, as shown in Fig. 5.[102]

A layered doped sol–gel sample, doped with FULP, has been investigated by the same method, the sample has two layers, each 100 mm thick, interleaved by a sodalime glass 150 mm thick, having $T_{lin} = 0.80$. Also this sample does not show any NL scattering effects (last panel in Fig. 5).

Experiments to confirm that C_{60} molecules embedded in inorganic sol–gel matrices are preserved and do not form detectable microcrystalline aggregates have been performed with Raman spectroscopy and X-ray diffraction (XRD) on a SiO_2–C_{60} sonogel based on tetraethylorthosilicate (TEOS) and tetramethylorthosilicate (TMOS) hydrolyzed in acidic conditions.[107] With Raman spectroscopy it has been verified that intact C_{60} is incorporated into the sol–gel glasses and that C_{60}

molecules feel an amorphous local environment. The Raman spectrum of a SiO_2–C_{60} sol–gel glass showed the same vibrational modes, in some cases slightly broader, than a pure C_{60} film on a SiO_2 substrate. In the case of XRD experiments the minimum detectability of crystalline C_{60} in SiO_2 has been estimated to be approximately 0.5 wt%. Since the C_{60} concentration in the sonogel was 1 wt%, the absence of sharp lines in the XRD signal of samples is a confirmation that no crystalline phases were detected in these doped glasses and C_{60} is microscopically dispersed through the glass.

Bentivegna et al. compared RSA properties of C_{60} doped xerogel to those in solution, by doping a sol based on vinyltriethoxysilane (VTES) with a benzene C_{60} solution.[108] The obtained OL performances, reported in Table 3, indicated that RSA characteristics were maintained when C_{60} is embedded in

Table 3 OL properties of polymeric and sol–gel matrices

Matrix	Fullerenes	Concentration/M	T_{lin} %	FOM (T_{lin}/T_{NL}) 532 nm	FOM (T_{lin}/T_{NL}) 690 nm	Damage threshold/J cm^{-2}	Ref.
PMMA	**8**	1.75×10^{-3}	92	—	2.5	11.5	81
PMMA 1.7 mm	**C_{60}**	0.06 wt%	69	2.8	—	1.2–1.8	80
PMMA 0.1 mm	**Methano-C_{60}**	5.9×10^{-4}	80	1.6	—	0.6	92
PMMA 0.4 mm	**Methano-C_{60}**	$0.6–1.0 \times 10^{-3}$	22 ÷ 79	1.6–7.3	—	1.2	92
SiO_2	**C_{60}**	0.3 wt%	< 10	2.5	—	6–7	87
Polystyrene 1 mm	**C_{60}**	0.2 wt%	20	3.5	—	0.6	48
SiO_2 sonogel	**C_{60}**	1 wt%	3 ÷ 14	10–4	—	> 1	107
SiO_2 sonogel	**PCBCR**	—	20	2.9	—	> 10	110
SiO_2 not porous	**PCBM**	—	70	1.6	—	> 10	111
MTES/VTES xerogel 1 mm	**C_{60} Derivative**	—	30	12	—	> 10	109
VTES xerogel 1 mm	**C_{60}**	1.4×10^{-4}	45	7.5	—	> 2	108
Composite TEOS–MMA	**C_{60} BBTDOT**	0.5–1 wt%	30	—	—	2.5–3	113
GPTMS-TiCl$_4$	**8**	2.0×10^{-3}	83	—	6.2	11.2	81,82
GPTMS-Zr	**8**	2.8×10^{-3}	79	—	6	15–30	81,82
GPTMS-BF$_3$	**8**	3.3×10^{-3}	79	—	> 7.6	> 15	81,82
GPTMS-Zr 0.62 mm	**8**	7.4×10^{-3}	63	—	25	—	102,104
GPTMS-Zr	**8**	2.8×10^{-3}	52	—	11–65^a	15–30	103
GPTMS-Zr MULTILAYERS (total thickness 2150 µm)							
10 layers, 500 µm layer^{-1}	**8**	8.1×10^{-3}	77	—	7.7	—	102,104
2 layers, 100 µm layer^{-1}	**8**	2.0×10^{-3}	90	—	6.9	—	102,104
4 layers, 200 µm layer^{-1}	**8**	9.7×10^{-4}	90	—	4.5	—	102,104
6 layers, 600 µm layer^{-1}	**8**	3.9×10^{-4}	90	—	3.3	—	102,104
2 layers, 100 µm layer^{-1}	**8**	5.6×10^{-3}	82	—	2.2	3.2–32	103
2 layers, 100 µm layer^{-1}	**8**	5.6×10^{-3}	87	—	12.5^a	3.2–32	103

^{a}Fast focusing optics.

xerogel matrices, with the only difference that the ground state absorption cross section slightly decreases and the ground state absorption recovery time increases from 50 ps to 270 ps. In other experiments organically modified xerogels have been doped with functionalized fullerenes.[109] Multifunctionalized fullerenes have been obtained by a nucleophilic addition of 3-aminopropyltriethoxysilane (APTES) to the C_{60}/C_{70} double bonds. This derivative APTES solution was added to a sol prepared by acid-catalyzed hydrolysis of a methyl (MTES) or VTES, and the gelification occurred in a few minutes due to the addition of the APTES solution. Bulk samples 1.5 mm thick were obtained after gelification and drying at 40 °C. As the authors remarked, grafting strongly perturbs, in a detrimental way, the RSA characteristics at 532 nm in the nanosecond regime, even if it could be a way of optimizing performances at a given wavelength.

A further demonstration that the sol–gel glass contains C_{60} in a molecular dispersion has been obtained by comparing relaxation dynamics of the excited-state absorption at several wavelengths for C_{60} in solution, thin films and inorganic sol–gel matrix.[110,111] The results indicated that the dynamics of fullerene solid thin films show a rapid decay < 20 ps of the excited state, while in C_{60} bulk glasses they occur on a long timescale (lifetime of the order of 5 ns), the bulk dynamics resemble that of a solution where a molecular dispersion of fullerene occurs. The excited state time is sufficiently long enough to allow the presence of a consistent intersystem crossing process, occurring in a time of about 600 ps, and explaining the OL behavior, with ns pulses, *via* RSA (Fig. 6).

As in the case of generally used procedures, a fullerene solution is added to a previously prepared alkoxide sol; in the work of McBranch *et al.*,[110] sonication was found to be an effective method to disrupt C_{60} aggregates within the sol both in the step of dissolving C_{60} and during the step of mixing the C_{60} solution with the sol; at the same time, sonication accelerates the rate of hydrolysis of the alkoxide precursor. However, a crucial point was the use of a suitable solvent for fullerene, toluene in this case, that has to be added to the sol before the addition of the C_{60} solution, to avoid cavitation effects produced by ultrasound waves. Different strategies were followed to embed pure C_{60} in sol–gel glasses and to overcome the strong tendency of fullerene to form aggregates. Preliminary OL results on sonogels doped with C_{60} show that samples are characterized by a relatively large amount of linear scattering typical of porous glasses. In fact, the same authors developed optimized procedures for curing and preparing the doped inorganic sol–gel glasses, obtaining controlled concentrations, high clarity and sufficient mechanical strength to have optical quality surfaces by polishing.[110,112] Other than a

Fig. 6 D_T/T at 750 nm *vs.* delay time (a) up to 2.5 ps, and (b) up to 0.5 ns, for C_{60} in toluene solution (solid circles), in sol–gel glasses (open squares), and in thin films (solid triangles). From ref. 110.

thermal treatment at 50 °C for several days, subsequent heat treatments were performed at 500 °C and 700 °C with a heating rate of 2° min^{-1}, generating a fully densified glass, in films, with thickness < 1 μm, and bulk shapes. C_{60} was added to the sols as saturated toluene or monochlorobenzene solution and, as the authors stress, it was important that the same sol–gel compatible solvent was added to the sol before the addition of the C_{60} saturated solution, in order to avoid cluster formation in the final glass.

Singly-derivatized methanofullerenes (phenyl-C_{61}-butyric acid cholestryl ester, PCBCR and 1-(3-methoxycarbonyl)propyl-1-phenyl-[6,6]-C_{61}, PCBM) have also been used by McBranch *et al.*[110,111] These soluble C_{60} derivatives have been found to allow the preparation of clear and uncracked monoliths, having greater mechanical strength and greater ability to withstand heat treatment. OL results on these optimized glasses were obtained in a large region, between 532 and 700 nm, and no damage was seen at the highest pulse energy available at 700 nm.

Very different materials have been prepared through the sol–gel process by Prasad *et al.*[113,114] They produced composite glasses, consisting of many phases separated on a nanometric scale. The monolith silica gel, doped with fullerene, is prepared highly porous, with pores in the nanoscale region. These pores are filled with methyl methacrylate (MMA) which is then polymerized.[115] By this method, bulk materials having high optical quality (loss ≈ 1 dB m^{-1}) and large size can be produced. To make multifunctional bulk materials, in which different optically responsive materials reside in different phases, a multistep impregnation method has been used. The prepared porous glasses were placed in saturated C_{60} toluene solution (the final C_{60} concentration was 0.5 wt% with respect to SiO_2), placed on a hot plate at 125 °C and then immersed in an MMA monomer solution catalyzed for full polymerization; the MMA solution in this case contains the organic dye, bisbenzothiazole 3,4-didecyloxythiophene (BBTDOT). The OL properties of the C_{60} and C_{60}-BBTDOT doped nanocomposites have been measured at 532 and 800 nm. C_{60} is more active as an optical limiter at 532 nm than at 800 nm and the suggested mechanism is RSA owing to one photon absorption. BBTDOT shows a linear absorption maximum at 400 nm, with input pulses at 800 nm and a high intensity two photon absorption process is induced and confirmed from the presence of the induced blue fluorescence; the BBTDOT sample shows higher absorption at 800 nm than at 532 nm. The codoped sample shows excellent OL behavior both at 532 nm and 800 nm. The NL behavior at 532 nm is slightly enhanced compared with the OL of the sample doped only with C_{60}, suggesting a contribution from BBTDOT. On the contrary, at 800 nm the NL effect is slightly lower with respect to the BBTDOT alone, probably due to the linear absorbance of C_{60} that decreases the local intensity and so the NL absorption of BBTDOT.

A summary of the OL properties of some of the more significant experiments in solid matrices is reported in Table 3, together with main results of the University of Padova group. This table reports different fullerenes, from pristine C_{60} to different fullerene derivatives, in polymeric and sol–gel matrices, with the obtained concentration, the linear transmittances (T_{lin}), the FOMs and damage thresholds (D_T). The determination of the exact final molar concentration of fullerene in solid sol–gel matrices is not simple. In the case of sol–gel samples, especially for hybrid matrices, a particular procedure has been developed to convert the molar ratio C_{60}/MO_2 (M = Si and/or Ti and/or B) to C_{60} molarity.[81] The first value is found by adding a controlled amount of C_{60} to a sol, in which the molar concentration of alkoxide is known. When the xerogel is obtained, the density of the material (g cm^{-3}) is measurable, but it is not convertible to the density (mol cm^{-3}). In fact, the stoichiometry of the molecule is not known because OH and organic residual groups are present. For this reason the
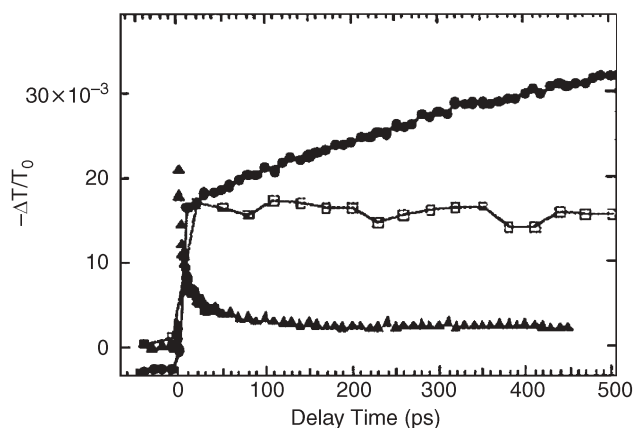
material is treated at 1200 °C; only the oxide MO_2 remains and it is directly correlated to the initial alkoxide content. Taking into account the weight loss, the density of MO_2 expressed in MO_2 cm^{-3} is calculated. This value permits conversion of the molar ratio $C_{60} : MO_2$ into C_{60} molar concentration.

The figures of merit (FOM) reported allow characterisation of the OL performances of samples, measured with different, but similar, experimental set-up. It is possible to observe that the largest FOM has been reached with the GPTMS-Zr bulk, doped with FULP. Similar performances have also been reached with multilayer structures, with 3 to 10 layers, prepared with the same GPTMS-Zr matrix.[102,103,106] These multilayer structures have been prepared by evaporating the solvent from the sols and depositing viscous sols just before gelation between sodalime slides of appropriate thickness. The doped layer thicknesses were controlled by appropriate spacers and OL characterization has been performed with a fast focusing system, which is likely to be used in practical protection devices.[102,116–119]

6.3 Laser damage threshold of NLO fullerene doped materials

An OL dye embedded in a solid matrix can be employed to design a protection device when its linear and nonlinear optical properties are preserved, after inclusion, and the matrix shows high resistance under high fluences of the input laser. It has already been demonstrated, in the previous section, that fullerene can be well incorporated in both polymeric and sol–gel matrices, without losing its optical properties. Damage thresholds of sol–gel samples have been, generally, evaluated by OL measurements, by slowly increasing and decreasing the input energy and carefully controlling the intensity and the shape of the transmitted beam. When a drastic and irreversible decrease in the transmitted beam is found, the sample is damaged. With a CCD camera it has been possible to obtain a detailed image of the damaged samples. Fig. 7 shows CCD pictures of the laser beam in a GPTMS-Zr bulk, doped with FULP, before and after damaging, with a slow focusing optic configuration. The image of the beam crossing the sol–gel sample is recorded at the beam-waist. Before damaging the intensity distribution of the beam is almost Gaussian, after damaging the beam seems to be cut in the center, where the sample has been damaged and a dark spot is visible.

Several D_T values, found in literature, have been reported in Table 3. The first value of D_T in a PMMA doped with C_{60} was
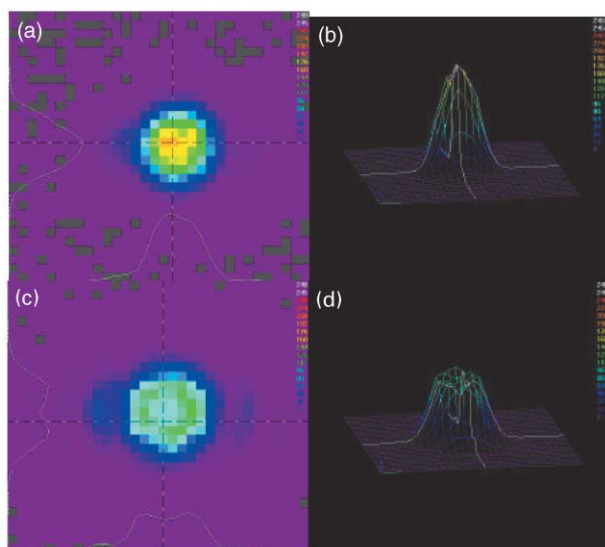
reported by Kost et al.[80] They observed that larger D_T values are obtained, by laterally translating samples during the measurements, indicating progressive damage of the PMMA under irradiation. Moreover, samples with different C_{60} concentrations showed the same D_T, indicating that the damage was due to PMMA properties, probably absorbing impurities. Experiments performed with tert-butyl methano-C_{60} carboxylate doped PMMA films, with different thicknesses, showed that thinner films, of 0.1 mm, were more fragile toward pulsed laser radiation, showing a $D_T \approx 0.6$ J cm^{-2}, with respect to thicker films, of 0.4 mm, with a $D_T \approx 1.2$ J cm^{-2}. The obtained D_T values were comparable to those obtained by Kost et al.[92] With a 1 mm thick polystyrene sample, doped with C_{60}, the D_T value still shows the same order of magnitude.[48]

In porous sol–gel nanocomposite materials, filled with MMA and doped with C_{60} and BBDOT, D_T reached a value of 2.5–3 J cm^{-2}.[113] This value was not attributed to an intrinsic damage threshold of the composite material but to the presence of particulate contaminants.

Larger D_T values, with respect to PMMA matrices, have been measured through different experiments in doped sol–gel matrices, when the sol–gel glasses were properly densified.

In the earlier works of McBranch et al. low laser damage thresholds, of about 1 J cm^{-2}, were found; in this case the sol–gel glasses were not fully densified.[107] In ref. 111 an increased D_T values of sol–gel samples has been observed: one order greater than polymeric samples. At 532 nm the damage threshold of sol–gels seems to increase with the fullerene concentration; the authors suggested that the local nonlinear absorption, before the focus position, may protect the sample in the focus.

Damage thresholds in sol–gel samples as high as 6–7 J cm^{-2} have been reached in SiO_2 and SiO_2–TiO_2 matrices, with 0.3 wt% fullerene concentration by G. Fuxi et al.[87] The highest damage threshold values have been obtained by the Padova group in GPTMS-Zr matrices doped with FULP.[82,103] These samples showed D_T values of between 15 and 30 J cm^{-2}, while in multilayer structures the D_T value was between 3.2 and 32 J cm^{-2}.[102,103]

It has been reported that the D_T value in elastomers is more than 600 times greater than its glassy thermosetting analog and over 20 times greater than PMMA.[120] This means that thermomechanical properties are important for improving laser damage resistance in organic polymers. These properties have been measured with GPTMS matrices: the elastic modulus has been correlated to the value of the D_T. It has been found that a lower rigidity gives larger D_T values. This effect is probably due to the better relaxation in the less rigid matrix of the thermal stress induced by the laser light. This is
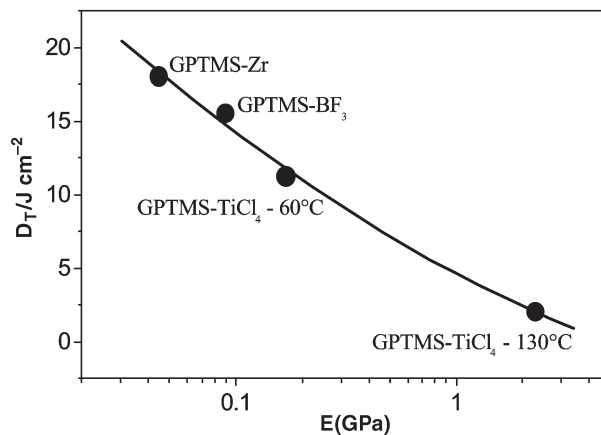

Fig. 7 CCD image and 3D intensity profile of the beam at the waist in a GPTMS-Zr sol–gel sample, $\lambda = 690$ nm. Panels (a) and (b) represent the beam before damaging. Panels (c) and (d) represent the beam after damage in the same sample, at the same input energy.

Fig. 8 Laser damage threshold (D_T) as a function of elastic modulus (E) of sol–gel samples doped with the same content of homogeneously dispersed FULP.

confirmed by observing data of Fig. 8, where the values of D_T are reported as a function of the elastic modulus, E: these samples possess the same content of FULP homogeneously dispersed.

7. Conclusions and outlook

The great potential of nanocomposite materials, whose optical properties depend on doping with fullerenes and fullerene derivatives, is demonstrated by the large variety of studies on this field herein reported. The necessity to develop a solid matrix is based on the feasibility of new desired optical devices, based on fullerenes, for potential industrial applications. Optical property studies of fullerene doped solid materials have been discussed very briefly, devoting particular regard to the observation of the modifications induced by the solid environment on the optical properties of fullerenes. From the reported works, it has been clearly observed that the final linear and nonlinear optical properties of fullerenes are strictly related to the matrix used for inclusion, to the possibility of functionalizing the pristine C_{60}, and to the processing protocol of the solid nanocomposite. The obtained optical properties are different from one process to another. For these reasons the development of fullerene doped solid devices, with high performances, should take into account the whole synthesis process, by completely monitoring the photophysical properties of the embedded material.

Acknowledgement

References

1 H. W. Kroto, J. R. Heath, S. C. O'Brien, R. F Curley and R. E. Smalley, *Science*, 1985, **318**, 162.
2 W. Krätschmer, L. D. Lamb, K. Fostiropoulos and D. R. Huffman, *Nature*, 1990, **347**, 354.
3 J. W Arbogast, A. P. Darmanyan, C. S. Foote, Y. Rubin, F. N. Diederich, M. M. Alvarez, S. J. Anz and R. L. Whetten, *J. Phys. Chem.*, 1991, **95**, 11.
4 J. Catalan and J. Elguero, *J. Am. Chem. Soc.*, 1993, **115**, 9249–9252.
5 R. V. Bensasson, T. Hill, C. Lambert, E. J. Land, S. Leach and T. G. Truscott, *Chem. Phys. Lett.*, 1993, **201**(1,2,3,), 326.
6 M. R. Fraelich and R. B. Weisman, *J. Phys. Chem.*, 1993, **97**, 11145.
7 H. T. Etheridge III, R. D. Averitt, N. J. Halas and R. B. Weisman, *J. Phys. Chem.*, 1995, **99**, 11306.
8 T. W. Ebbesen, K. Tanigaki and S. Kuroshima, *Chem. Phys. Lett.*, 1991, **181**(6), 501.
9 H. S. Nalwa and S. Miyata, *Nonlinear Optics of Organic Molecules and Polymers*, CRC Press Inc., Boca Raton, FL, USA, 1997.
10 L. W. Tutt and A. Kost, *Letters to Nature*, 1992, **356**, 225.
11 M. J. Rosseinsky, *J. Mater. Chem.*, 1995, **5**, 1497.
12 J. H. Schon, Ch. Kloch and B. Batlogg, *Nature*, 2000, **408**, 549.
13 N. S. Sariciftci, L. Smilowitz, A. J. Heeger and F. Wudl, *Science*, 1992, **258**, 1474.
14 R. V. Bensasson, E. Bienvenue, J.-M. Janot, S. Leach, P. Seta, D. I. Schuster, S. R. Wilson and H. Zhao, *Chem. Phys. Lett.*, 1995, **245**, 566.
15 R. M. Williams, J. M. Zwier and J. W. Verhoeven, *J. Am. Chem. Soc.*, 1995, **117**, 4093.
16 W. Ji, S. H. Tang, G. Q. Xu, H. S. O. Chan, S. C. Ng and W. W. Nh, *J. Appl. Phys.*, 1993, **74**(6), 3669.

17 H. Liu, W. Jia, F. Lin and S. Mao, *J. Luminesc.*, 1996, **66&67**, 128.
18 H. Liu, B. Taheri, W. Jia, F. Lin and S. Mao, *Appl. Phys. Lett.*, 1996, **68**(11), 1570.
19 P. A. Chollet and F. Kajzar, *J. Sol–gel Sci. Technol.*, 2001, **22**, 255.
20 P. Innocenzi and G. Brusatin, *Chem. Mater.*, 2001, **13**, 3126.
21 G. Agostini, L. Pasimeni, M. Ruzzi, S. Monti, M. Maggini, M. Prato, I. Lamparth and A. Hirsch, *Chem. Phys.*, 2000, **253**, 105.
22 M. Prato, *J. Mater. Chem.*, 1997, **7**, 1097.
23 A. G. Camp, A. Lary and W. T. Ford, *Macromolecules*, 1995, **28**, 7959.
24 D. Avnir, *Acc. Chem. Res.*, 1995, **28**, 328.
25 L. L. Hench and J. West, *Chem. Rev.*, 1990, **90**, 33.
26 C. Sanchez and B. Lebeau, *MRS Bulletin*, 2001, **May**, 377.
27 R. Gvishi, U. Narang, G. Ruland, D. N. Kumar and P. N. Prasad, *Appl. Organomet. Chem.*, 1997, **11**, 107.
28 D. Levy and L. Esquivias, *Adv. Mater.*, 1995, **7**(2), 120.
29 M. Maggini, C. De Faveri, G. Scorrano, M. Prato, G. Brusatin, M. Guglielmi, M. Meneghetti, R. Signorini and R. Bozio, *Chem-Eur. J.*, 1999, **5**(9), 2501.
30 R. Bozio, M. Meneghetti, R. Signorini, M. Maggini, G. Scorrano, M. Prato, G. Brusatin and M. Guglielmi, *Photoactive Organic Materials*, eds F. Kajzar, V. M. Agranovich and C. Y.-C. Lee, Kluwer Academic Publishers, Dordrecht, Netherlands, 1996, 159–174.
31 M. Maggini, G. Scorrano and M. Prato, *J. Am. Chem. Soc.*, 1993, **115**, 9798.
32 M. Prato, M. Maggini, G. Giacometti, G. Scorrano, G. Sandonà and G. Farnia, *Tetrahedron*, 1996, **52**, 5221.
33 A. Bianco, M. Maggini, G. Scorrano, C. Toniolo, G. Marconi, C. Villani and M. Prato, *J. Am. Ceram. Soc.*, 1996, **118**, 4072.
34 A. Bianco, F. Gasparrini, M. Maggini, D. Misiti, A. Polese, M. Prato, G. Scorrano, C. Toniolo and C. Villani, *J. Am. Ceram. Soc.*, 1997, **119**, 7550.
35 R. S. Ruoff, D. S. Tse, R. Malhotra and D. C. Lorents, *J. Phys. Chem.*, 1993, **97**, 3379.
36 Y. P. Sun, B. Ma, C. E. Bunker and B. Liu, *J. Am. Chem. Soc.*, 1995, **117**, 12705.
37 B. Kraaber, C. H. Lee, D. McBranch, D. Moses, N. S. Saricifci and A. J. Heeger, *Chem. Phys. Lett.*, 1993, **213**, 389.
38 R. Lascola and J. C. Wright, *Chem. Phys. Lett.*, 1997, **269**, 79.
39 Q. Gong, P. Yuan, Z. Xia, Y. H. Zou, J. Li, H. Yang, H. Hong, F. Yu, S. Chen, Z. Wu, X. Zhou and F. Li, *Solid State Commun.*, 1997, **103**(7), 403.
40 G. Ma, S. Qian, Y. Chen, R. Cai, W. Qian, L. Lin and Y. Zou, *SPIE*, 1999, **3798**, 140.
41 Y. Chen, Z. Huang, R. Cai, B. Yu, Y. Huang, Y. Su and Z. Wu, *Eur. Polym. J.*, 1998, **34**, 421.
42 M. Cha, N. S. Sariciftci, A. J. Heeger and J. C. Hummelen, *Appl. Phys. Lett.*, 1995, **67**(26), 3850.
43 N. V. Kamanina, L. N. Kaporskii, A. Leyderman, Y. Cui, V. Vikhnin and M. Vlasse, *Mol. Mater.*, 2000, **13**, 275.
44 N. V. Kamanina, I. V. Bagrov, I. M. Belousova, S. O. Kognovitskii and A. P. Zhevlakov, *Optics Commun.*, 2001, **194**, 367.
45 Y. A. Cherkasov, N. V. Kamanina, E. L. Alexandrova, V. I. Berendyaev, N. A. Vasilenko and B. V. Kotov, *SPIE*, 1998, **3471**, 254.
46 N. V. Kamanina, *Optics Commun.*, 1999, **162**, 228.
47 N. V. Kamanina and L. N. Kaporskii, *Non-Linear Optics*, 2001, **27**, 347.
48 Y. Kojima, T. Matsuoka, H. Takahashi and T. Kurauchi, *Macromol.*, 1995, **28**, 8868.
49 F. Yan, X. M. Bao and X. W. Wu, *Appl. Phys. Lett.*, 1995, **67**(23), 3471.
50 S. Y. Wang, W. Z. Shen, X. C. Shen, L. Zhu, Z. M. Ren and Y. F. Li, *Appl. Phys. Lett.*, 1995, **67**(6), 783.
51 G. Gu, W. Ding, Y. Du, H. Huang and S. Yang, *Appl. Phys. Lett.*, 1997, **70**(19), 2619.
52 G. Gu, W. Ding, G. Cheng, S. Zhang, Y. Du and S. Yang, *Chem. Phys. Lett.*, 1997, **270**, 135.
53 G. Gu, W. Ding, G. Cheng, W. Zang, H. Zen and Y. Du, *Appl. Phys. Lett.*, 1995, **67**(3), 326.
54 G. Gu, W. Ding, Y. Du, H. Huang and S. Yang, *Appl. Phys. Lett.*, 1997, **70**(19), 2619.
55 B. Hamilton, J. S. Rimmer, M. Anderson and D. Leigh, *Adv. Mater.*, 1993, **5**(7/8), 583.
56 A. Lambrate, J. M. Janot, L. C. de Ménorval, R. Backov, J. Rozière, J. L. auvajol, J. Allègre and P. Seta, *Synth. Met.*, 1999, **103**, 2426.
57 A. Lambrate, J. M. Janot, A. Elmidaoui, P. Seta, L. C. de

Ménorval, R. Backov, J. Rozière, J. L. Sauvajol and J. Allègre, *Chem. Phys. Lett.*, 1998, **295**, 257.

58 D. Wang, J. Zuo, Q. Zhang, Y. Luo, Y. Ruan and Z. Wang, *J. Appl. Phys.*, 1997, **81**(3), 1413–1416.

59 C. Zhang, X. Xiao, W. Ge, M. M. Loy, W. Dazhi, Z. Qujin and Z. Jian, *Appl. Phys. Lett.*, 1996, **68**(7), 943.

60 H. Zeng, Z. Sun, Y. Segawa, F. Lin, S. Mao and Z. Xu, *J. Appl. Phys.*, 2001, **89**(11), 6539.

61 H. Zeng, Z. Sun, Y. Segawa, F. Lin, S. Mao and Z. Xu, *J. Phys. D*, 2001, **34**, 1.

62 H. Zeng, Z. Sun, Y. Segawa, F. Lin, S. Mao, Z. Xu and S. H. Tang, *J. Phys. D*, 2000, **33**, L93.

63 L. Zhu, L. Y. Li, J. Wang and J. Shen, *Chem. Phys. Lett.*, 1995, **239**, 393.

64 J. Shen, J. Wang, B. Zhou, Z. Deng, Z. Wenig, L. Zhu, L. Zhao and Y. Li, *J. Non-Cryst. Sol.*, 1998, **225**, 315.

65 L. Zhu, Y. Li, J. Wang and J. Shen, *J. Appl. Phys.*, 1995, **77**(6), 2801.

66 L. Zhu, P. Ong, J. Shen and J. Wang, *J. Phys. Chem. Sol.*, 1998, **59**, 819.

67 B. Zhou, J. Wang, L. Zhao, J. Shen, Z. Deng and Y. Li, *J. Vac. Sci. Technol. B*, 2001, **18**(4), 2000.

68 I. Hasegawa, K. Shibusa, S. Kobayashi, S. Nonomura and S. Nitta, *Chem. Lett.*, 1997, 995.

69 T. Ohno, K. Matsuishi and S. Onari, *J. Chem. Phys.*, 2001, **114**(21), 9633.

70 T. Ohno, K. Matsuishi and S. Onari, *J. Appl. Phys.*, 1998, **83**(9), 4939.

71 D. Felder, D. Guillon, R. Levy, A. Mathis, J. F. Nicoud, J. F. Nierengarten, J. L. Rehspringer and J. Schell, *J. Mater. Chem.*, 2000, **10**, 887.

72 J. Schell, D. Felder, J. F. Nierengarten, J. L. Rehspringer, R. Lévy and B. Hönerlage, *J. Sol–gel Sci. Technol.*, 2001, **22**, 25.

73 G. Brusatin, M. Guglielmi, R. Bozio, M. Meneghetti, R. Signorini, M. Maggini, G. Scorrano and M. Prato, *J. Sol–gel Sci. Technol.*, 1997, **8**, 609.

74 G. Brusatin and P. Innocenzi, *J. Sol–gel Sci. Technol.*, 2001, **22**, 189.

75 M. Prato, M. Maggini, G. Scorrano, G. Brusatin, P. Innocenzi, M. Guglielmi, M. Meneghetti and R. Bozio, *«Science and Technology of Fullerene Materials», Mater. Res. Symp. Proc.*, 1995, **359**, 351–356.

76 M. Maggini, G. Scorrano, M. Prato, G. Brusatin, P. Innocenzi, M. Guglielmi, M. Meneghetti and R. Bozio, *Electrochem. Soc. Proced.*, 1995, **95–10**, 84–89.

77 M. Maggini, G. Scorrano, M. Prato, G. Brusatin, P. Innocenzi, M. Guglielmi, A. Renier, R. Signorini, M. Meneghetti and R. Bozio, *Adv. Mater.*, 1995, **7**(4), 404.

78 M. Meneghetti, R. Signorini, M. Zerbetto, R. Bozio, M. Maggini, G. Scorrano, M. Prato, G. Brusatin, E. Menegazzo and M. Guglielmi, *Synth. Met.*, 1997, **86**, 2353.

79 M. Meneghetti, R. Signorini, S. Sartori, R. Bozio, M. Maggini, G. Scorrano, M. Prato, G. Brusatin and M. Guglielmi, *Synth. Met.*, 1999, **103**, 2474.

80 A. Kost, L. Tutt, M. B. Klein, T. K. Dougherty and W. E. Elias, *Opt. Lett.*, 1993, **18**, 334.

81 G. Brusatin, M. Guglielmi, P. Innocenzi, R. Bozio, R. Signorini, M. Meneghetti, M. Maggini, G. Scorrano and M. Prato, *SPIE*, 1999, **3803**, 90.

82 G. Brusatin, P. Innocenzi, M. Guglielmi, R. Signorini and R. Bozio, *Non-Linear Optics*, 2001, **27**, 259.

83 P. Innocenzi, G. Brusatin, M. Guglielmi, R. Signorini, R. Bozio and M. Maggini, *J. Non-Cryst. Sol.*, 2000, **256**, 68.

84 G. Brusatin, P. Innocenzi, M. Guglielmi, R. Signorini, M. Meneghetti, R. Bozio, M. Maggini, G. Scorrano and M. Prato, *J. Sol–gel Sci. Technol.*, 2000, **19**, 263.

85 R. Signorini, M. Meneghetti, R. Bozio, G. Brusatin, P. Innocenzi, M. Guglielmi and F. Della Negra, *J. Sol–gel Sci. Technol.*, 2001, **22**, 245.

86 J. Schell, D. Ohlmann, D. Brinkmann, R. Levy, M. Joucla, J. L. Rehspringer and B. Honerlage, *J. Chem. Phys.*, 1999, **111**(13), 5929.

87 Z. Congshan, X. Haiping and G. Fuxi, *Proc. Of XVIII Int. Congr. On Glass*, 1995, **4**, 204.

88 V. P. Belousov, I. M. Belousova, V. P. Budtov, V. V. Danilov, O. B. Danilov, A. G. Kalintsev and A. A. Mak, *J. Opt. Technol.*, 1997, **64**, 1081.

89 M. Ouyang, K. Z. Wang, H. X. Zhang, Z. Q. Xue, C. H. Huang and D. Qiang, *Appl. Phys. Lett.*, 1996, **68**, 2441.

90 K. Hosoda, K. Tada, M. Ishikawa and K. Yoshino, *Jpn. J. Appl. Phys., Part 2*, 1997, **36**, L372.

91 Y. Song, X. Bao, X. Yang, X. Zhang and R. Wang, *Proc. SPIE*, 1996, **2854**, 230.

92 Y. P. Sun, G. E. Lawson, J. E. Riggs, B. Ma, N. Pung and D. K. Moton, *J. Phys. Chem. A*, 1998, **102**, 5520.

93 J. E. Riggs and Y. P. Sun, *J. Phys. Chem. A*, 1999, **103**, 485.

94 Z. Lu, S. H. Goh, S. Y. Lee, X. Sun and W. Ji, *Polymer*, 1999, **40**, 2863.

95 Y. Kojima, T. Matsuoka, H. Takahashi and T. Kurauchi, *J. Mater. Sci. Lett.*, 1997, **16**, 2029.

96 Y. Kojima, T. Matsuoka, H. Takahashi and T. Kurauchi, *J. Mater. Sci. Lett.*, 1997, **16**, 999.

97 Y. P. Sun and J. E. Riggs, *J. Chem. Faraday Trans.*, 1997, **93**(10), 1965.

98 J. Schell, D. Ohlmann, B. Hönerlage, R. Levy, M. Joucla, J. L. Rehspringer, J. Serughetti and C. Bovier, *Carbon*, 1998, **36**(5–6), 671.

99 J. Schell, D. Felder, J. F. Nierengarten, J. L. Rehspringer, R. Lévy and B. Hönerlage, *J. Sol–gel Sci. Technol.*, 2001, **22**, 25.

100 I. M. Belusova, V. P. Belusov and O. B. Danilov, *Non-Linear Optics*, 2001, **27**, 219.

101 I. M. Belusova, V. P. Belusov, O. B. Danilov, V. V. Danilov, A. I. Sidorov and I. L. Yachnev, *Non-Linear Optics*, 2001, **27**, 233.

102 R. Signorini, M. Meneghetti, R. Bozio, M. Maggini, G. Scorrano, M. Prato, G. Brusatin, P. Innocenzi and M. Guglielmi, *Carbon*, 2000, **38**, 1653.

103 R. Signorini, A. Tonellato, M. Meneghetti, R. Bozio, M. Prato, M. Maggini, G. Scorrano, G. Brusatin, P. Innocenzi and M. Guglielmi, *Non-Linear Optics*, 2001, **27**, 193.

104 R. Signorini, M. Zerbetto, M. Meneghetti, R. Bozio, M. Maggini, C. DeFaveri, M. Prato and G. Scorrano, *Chem. Commun.*, 1996, 1981.

105 R. Signorini, M. Meneghetti, R. Bozio, M. Maggini, G. Scorrano, M. Prato, G. Brusatin and P. Innocenzi, in: *Multiphoton and Light Driven Multielectron Process in Organics: New Phenomena, Materials and Applications*, eds, F. Kajzar and M. V. Agranovich, Kluwer Academic Publishers, Dordrecht, Netherlands, 2000, 83.

106 R. Signorini, S. Sartori, M. Meneghetti, R. Bozio, M. Maggini, G. Scorrano, M. Prato, G. Brusatin and M. Guglielmi, *Nonlinear Optics*, 1999, **21**, 143.

107 D. McBranch, B. R. Mattes, A. Koskelo, J. M. Robinson and S. P. Love, *Proc. SPIE*, 1994, **2284**, 15.

108 F. Bentivegna, M. Canva, P. Georges, A. Brun, F. Caput, L. Malier and J. P. Boilot, *J. Appl. Phys. Lett.*, 1993, **62**, 1721.

109 M. Brunel, M. Canva, A. Brun, F. Chaput, L. Malier and J. P. Boilot, *Proc. MRS*, eds. R. Crane, K. Lewis, E. VanStryland and M. Khoshnevisan, 1995, **374**, 281.

110 L. Smilowitz, D. McBranch, V. Klimov, M. Grigorova, J. M. Robinson, B. J. Weyer, A. Koskelo, B. R. Mattes, H. Wang and F. Wudl, *Synth. Met.*, 1997, **84**, 931.

111 D. McBranch, V. Klimov, L. Smilowitz, M. Grigorova and B. R. Mattes, *Proc. SPIE*, 1996, **2854**, 140.

112 B. R. Mattes, D. W. McBranch, J. M. Robinson, S. P. Love and A. C. Koskelo, *U. S. Patent 5420081*, 1995.

113 R. Gvishi, J. D. Bhawalkar, N. D. Kumar, G. Ruland, U. Narang and P. N. Prasad, *Chem. Mater.*, 1995, **7**(11), 2199.

114 R. Gvishi, G. S. He, P. N. Prasad, U. M. Narang, F. V. Bright, B. A. Reinhardt, J. C. Rhatt and A. G. Dillard, *Appl. Spectrosc.*, 1995, **49**, 834.

115 E. J. A. Pope, M. Asami and J. D. Mackenzie, *J. Mater. Res.*, 1989, **4**, 1018.

116 P. A. Miles, *Appl. Opt.*, 1994, **33**(30), 6965.

117 D. J. Hagan, T. Xia, A. Dogariu, A. A. Said and E. W. Van Stryland, *Mat. Res. Soc. Symp. Proc.*, 1995, **374**, 161.

118 D. J. Hagan, T. Xia, A. Dogariu, A. A. Said and E. W. Van Stryland, *Appl. Opt.*, 1997, **36**(18), 4110.

119 P. A. Miles, *Appl. Opt.*, 1999, **38**(3), 566.

120 M. E. De Rosa, W. Su, D. Krein, M. C. Brant and D. G. McLean, *Proc. SPIE*, 1997, **3146**, 134.

121 R. Signorini, M. Zerbetto, M. Meneghetti, R. Bozio, M. Maggini, G. Scorrano, M. Prato, G. Brusatin, E. Menegazzo and M. Guglielmi, *«Fullerenes and Photonics III», Proc. SPIE*, 1996, **2854**, 130.